Motion Segmentation

Determination of Optical Flow and its Discontinuities using Non-Linear Diffusion

M. Proesmans[1], L. Van Gool[1], E. Pauwels[1], A. Oosterlinck[1]

ESAT-MI2, Katholieke Universiteit Leuven,
K. Mercierlaan 94, B-3001 Leuven, Belgium

Abstract. A new method for optical flow computation by means of a coupled set of non-linear diffusion equations is presented. This approach integrates the classical differential approach with the correlation type of motion detectors. A measure of inconsistency within the optical flow field which indicates optical flow boundaries. This information is fed back to the optical flow equations in a non-linear way and allows the flow field to be reconstructed while preserving the discontinuities. The whole scheme is also applicable to stereo matching. The model is applied to a set of synthetic and real image sequences to illustrate the behaviour of the coupled diffusion equations.

1 Introduction

Most methods for computing motion fields rely on spatial and temporal gradients of the image intensity. Since the optical flow problem is ill-posed, additional constraints are required. The simplest is the quadratic smoothness constraint [5]. Other constraints have been introduced using higher order spatial and temporal derivatives [6]. Some methods use overconstrained systems of equations [3, 14], rather than functional descriptions. Other methods try to look for specific features - such as corners [7]. It is a problem not to enforce smoothness of the flow field across flow discontinuities. Part of the problem lies in the required size of the operator masks to estimate the spatio-temporal derivatives of the grayvalue distribution. Large masks may be called for in order to eliminate the effect of noise, and to handle relatively large interframe distances. The method presented in this paper offers an alternative solution which roughly consists of three parts.

- Basically, the method starts from the differential approach of the optical flow problem.
- Unlike other differential methods, our approach is provided with a mechanism very similar to the matching process of correlation based approaches [11]. This mechanism allows for a dual implementation and inconsistencies within the resulting scheme turn out to be concentrated nearby flow discontinuities.
- Finally, the discontinuity information is fed back to the original optical flow scheme in a non-linear way in order to reconstruct the optic flow field while preserving its discontinuities.

Lecture Notes in Computer Science, Vol. 801
Jan-Olof Eklundh (Ed.)
Computer Vision – ECCV '94

2 Optical Flow

The classical differential techniques used for computation of optical flow are based on the image flow constraint equation.

$$I_x.u + I_y.v + I_t = 0 \ .$$

This equation relates spatio-temporal intensity changes to the velocity (u, v). It states that the image irradiance remains constant during the motion process. This single equation cannot fix the two motion components. Therefore most techniques use some kind of smoothness constraint such as introduced by Horn & Schunck [5] which led to the following minimizing functional

$$E = \int\int (\lambda(I_x.u + I_y.v + I_t) + (u_x^2 + u_y^2 + v_x^2 + v_y^2))dxdy \ .$$

Its main advantage is its simplicity, since minimizing the functional leads to a set of linear equations. In fact the corresponding evolution equations are

$$\begin{aligned} \frac{\partial u}{\partial t} &= \nabla^2 u - \lambda I_x(I_x.u + I_y.v + I_t) \\ \frac{\partial v}{\partial t} &= \nabla^2 v - \lambda I_y(I_x.u + I_y.v + I_t) \ . \end{aligned} \tag{1}$$

The smoothness constraint thus allows to estimate both velocity components, yet also forces the estimated vector field to vary smoothly across boundaries. A number of methods have been introduced [1, 6, 4, 10] to allow the optical flow field to be discontinuous, by appropriately exploiting the gradient information of the flow field. Nevertheless, the original Horn & Schunck scheme did not loose its popularity since its performance is quite satisfactory [2, 15] and this all the more in view of its simplicity. In the next sections, an alternative way of detecting discontinuities in the flow field will be derived.

3 The Dual Optical Flow Scheme

Since the optical flow equation relates spatio-temporal derivatives in a point, it can only hold locally. If accurate results are required for larger velocities, the gradient information has to be estimated with larger operator masks, resulting in a further degradation of discontinuities in the flow field. The method to be expounded, on the other hand, is bi-local.
Consider a point (x, y) in a frame at time t, for which we have some velocity estimates $(\tilde{u}, \tilde{v})$, and a point $(x - \tilde{u}dt, y - \tilde{v}dt)$ in a previous frame at time $t - dt$. For the 1D case, assuming an estimate $\tilde{u} = \frac{d\tilde{x}}{dt}$, we could rewrite the optical flow constraint as follows

$$\frac{dI}{dt} = I_x.u + I_t = 0$$

$$I_x.u + \frac{I(x,t) - I(x,t-dt)}{dt} = 0$$

$$I_x.u + \frac{I(x,t) - I(x - \tilde{u}dt, t - dt)}{dt} + \frac{I(x - \tilde{u}dt, t - dt) - I(x, t - dt)}{dt} = 0$$

and using the approximations

$$\begin{aligned} I(x - \tilde{u}dt, t - dt) &= I(x,t) - \tilde{u}I_x dt - I_t dt \\ I(x, t - dt) &= I(x,t) - I_t dt \end{aligned}$$

$$I_x(u - \tilde{u}) + \frac{I(x,t) - I(x - \tilde{u}dt, t - dt)}{dt} = 0 \ . \tag{2}$$

This *residual optical flow* equation yields – if we were able to estimate the intensity variations at a shifted location $x - \tilde{u}dt$ at time $t - dt$ – the residual velocity $u - \tilde{u}$. Figure 1 depicts more clearly the relationship between the different components in equation 2. Note that if $\tilde{u}$ were the real velocity u, the constraint would reduce to $I(x,t) - I(x - dx, t - dt) = 0$ which agrees with the constant irradiance assumption.

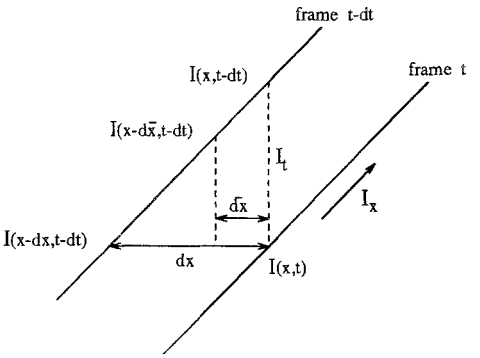

Fig. 1. interpretation of 1D optic flow equation

In two dimensions, the constraint equation yields

$$I_x u + I_y v + \mathbf{I}_t(\tilde{u}, \tilde{v}) = 0 \ , \quad \mathbf{I}_t(\tilde{u}, \tilde{v}) = -I_x \tilde{u} - I_y \tilde{v} + \frac{I(x,y,t) - I(x - \tilde{u}dt, y - \tilde{v}dt, t - dt)}{dt} \ . \tag{3}$$

If we introduce this constraint into the original evolution equations (1), we would end up with the following scheme

$$\begin{aligned} \frac{\partial u}{\partial t} &= \nabla^2 u - \lambda I_x (I_x u + I_y v + \mathbf{I}_t(\tilde{u}, \tilde{v})) \\ \frac{\partial v}{\partial t} &= \nabla^2 v - \lambda I_y (I_x u + I_y v + \mathbf{I}_t(\tilde{u}, \tilde{v})) \ . \end{aligned} \tag{4}$$

In the most general case $(\tilde{u}, \tilde{v})$ can be any estimate of the velocity components, From a practical point of view, they are chosen to be the estimates of the previous iteration. The resulting scheme is quite similar to correlation-based approaches, since a matching point is assigned to each point in the reference frame, based on equality of intensity.

Up to now the estimates $(\tilde{u}, \tilde{v})$ have been used to allocate a position in a previous frame. Similarly, one can start from the previous frame and search the corresponding point $(x + \tilde{u}dt, y + \tilde{v}dt)$ in the next frame. At first glance both schemes – forward and backward – seem to be equivalent, but they are not! In fact, nearby optical flow boundaries and occluding regions large inconsistencies between the two schemes are found. This characteristic can be used to create a motion edge indicator.

4 Discontinuities and Non-Linear Diffusion

4.1 Detection of discontinuities in the flow field

For the main part of the flow field, the dual scheme is consistent, i.e. they yield the same result. For two frames a and b, this means that

$$\mathbf{v}_a(x, y) = -\mathbf{v}_b(x - u_a\Delta t, y - v_a\Delta t) \text{ and } \mathbf{v}_b(x, y) = -\mathbf{v}_a(x - u_b\Delta t, y - v_b\Delta t)$$

with $\mathbf{v}_a = (u_a, v_a)$ and $\mathbf{v}_b = (u_b, v_b)$. Note that the velocity estimates in both schemes will be opposite to each other, since the roles of the frames are reversed. In the neighbourhood of discontinuities, the dual scheme is very likely to be inconsistent. Indeed, for a number of points in frame a, one can not find matching points in frame b, and vice versa, when they are occluded by the moving object. Using the difference vectors

$$\mathbf{C}_a = \mathbf{v}_a(x, y)+\mathbf{v}_b(x-u_a\Delta t, y-v_a\Delta t) \text{ and } \mathbf{C}_b = \mathbf{v}_b(x, y)+\mathbf{v}_a(x-u_b\Delta t, y-v_b\Delta t)$$

one can define inconsistency measures c_a and c_b which can be fed back to the dual optical flow scheme. In order to make them less sensitive to noise and independent of the velocity magnitude, an additional diffusion process is used:

$$\frac{\partial c}{\partial t} = \rho\nabla^2 c - \frac{c}{\rho} + 2\alpha(1 - c)||\mathbf{C}||$$

following Shah's [12] procedure for generating edge maps from intensity gradients. In this expression c indicates the likelihood of there being an edge at some position in the flow field. Hence, c is assumed to be smooth and close to 1 in the vicinity of a flow boundary, and close to zero away from such discontinuities.

4.2 Measures to prevent blurring of flow discontinuities

The smoothing process in the equations 4, which risk to blur the discontinuities in the optical flow field, can be controlled by introducing non-linear diffusion terms. Perona & Malik [9] proposed a method to locally sharpen edges in gray-value images, in order to preserve contrast. This can be achieved by making the diffusion coefficient γ dependent on the gray-level f

$$\frac{\partial f}{\partial t} = div(\gamma(f)\nabla f) \ .$$

Choosing $\gamma = 0$ at the boundaries and $\gamma = 1$ elsewhere, encourages smoothing within the regions but attenuates smoothing across the boundaries. Since the boundaries are not known yet, one chooses γ locally as a function of the gradient: $\gamma(f) = \gamma(\| \nabla f \|)$. Possible functions are

$$\gamma(f) = e^{-(\|\nabla f\|/K)^2} \quad \text{and} \quad \gamma(f) = \frac{1}{1 + (\|\nabla f\|/K)^2} \ .$$

Introducing a similar edge sharpening process into the optical flow equations will prevent smoothing across inconsistent regions. However, there are some serious shortcomings. The effect of the non-linearity is that smoothing is prohibited at each point containing inconsistent values. During the iteration process, velocity components can be inconsistent temporarily, especially if local gradient information is not consistent with the direction of the optical flow. If so, these components are restrained from converging to their correct values since any communication with neighbouring velocities is restricted. What we really need is a process which prevents consistent regions to suffer interference from inconsistent ones. This can be formulated mathematically by a diffusion coefficient γ which is weighted over a region of interest Ω, e.g.

$$\frac{\partial u}{\partial t} = div(\gamma(c)\nabla u) \ldots \ , \ \gamma(c) = \frac{\xi}{1 + (\frac{c}{K})^2} \text{ with } \xi \text{ such that } \int_{\Omega} \gamma(c) = 1 \ .$$

5 Integration

If we integrate all of the above ideas, we have a system of 6 coupled diffusion maps, four of which describe optical flow constraints, while the other two measure the consistency of the dual scheme. A bloack scheme of this algorithm is visualized in figure 2. These maps undergo a coupled development towards an equilibrium state.

$$\begin{aligned}
\tfrac{\partial u_1}{\partial t} &= div(\gamma(u_1)\nabla u_1) - \lambda I_x(I_x u_1 + I_y v_1 + \mathbf{I}_t(\tilde{u_1}, \tilde{v_1})) \ , \\
\tfrac{\partial v_1}{\partial t} &= div(\gamma(v_1)\nabla v_1) - \lambda I_y(I_x u_1 + I_y v_1 + \mathbf{I}_t(\tilde{u_1}, \tilde{v_1})) \ , \\
\tfrac{\partial u_2}{\partial t} &= div(\gamma(u_2)\nabla u_2) - \lambda I_x(I_x u_2 + I_y v_2 + \mathbf{I}_t(\tilde{u_2}, \tilde{v_2})) \ , \\
\tfrac{\partial v_2}{\partial t} &= div(\gamma(v_2)\nabla v_2) - \lambda I_y(I_x u_2 + I_y v_2 + \mathbf{I}_t(\tilde{u_2}, \tilde{v_2})) \ , \\
\tfrac{\partial c_1}{\partial t} &= \rho\nabla^2 c_1 - \tfrac{c_1}{\rho} + 2\alpha(1 - c_1)||\mathbf{C}_1(u_1, v_1, u_2, v_2)|| \ , \\
\tfrac{\partial c_2}{\partial t} &= \rho\nabla^2 c_2 - \tfrac{c_2}{\rho} + 2\alpha(1 - c_2)||\mathbf{C}_2(u_1, v_1, u_2, v_2)|| \ .
\end{aligned} \tag{5}$$

The iteration process proceeds by updating the above equations, and at the same time, recomputing the spatio-temporal information. The latter has been carried out by simple truncation of the shifted coordinates or by bilinear interpolation. In case of truncated coordinates, however, one can expect to observe oscillatory behaviour of the iterative scheme especially nearby flow discontinuities. The bilinear interpolation approach on the other hand converges much more smoothly, be it at a higher computational cost.

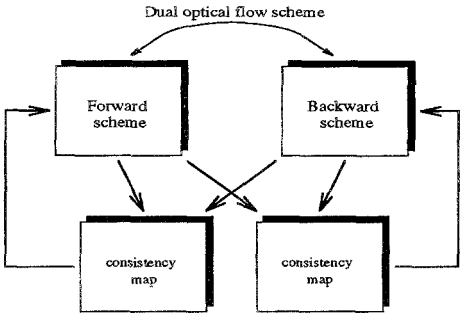

Fig. 2. Dual optical flow scheme with feed back loops

6 Stereo Matching

Stereo matching can be considered to be a special case of this optical flow scheme. In preliminary experiments, excluding vergence and occulo-torsion, the simplifying assumption was made that the disparities can be found as purely horizonal shifts (i.e. disparity $d = u$) and the v-maps were suppressed. This results in a system of 4 coupled diffusion equations which is reminiscent of a stereo approach proposed by Shah [13] who considers gradients instead of inconsistency measures.

7 Experimental Results

We applied the algorithm to a set of non-trivial synthetic image sequences which consist of a textured object moving on an identically textured background. The object can only be discriminated from the background by the motion cue. Figure 3 shows a circle translating diagonally at $3,5$ pixels/frame. The operator mask is 3×3, which is small compared to a real velocity of about 3.5 pixels/frame. The classical Horn & Schunck approach, although able to extract the optic flow field, shows clear distorsions in the flow field for these small mask sizes. The dual approach (figure 4) succeeds in finding the correct displacement field. Each of the inconsistency images contains part of the information concerning flow boundaries or occluding regions. The latter can be observed as a thickening of the boundary contours. The left image shows the region which is about to become visible, while the right image contains the region which is going to be occluded. It is interesting to note that these data can be rearranged into a boundary image δ and an occluded region image ω.

$$\delta = min(c_1, c_2) \text{ and } \omega = max(c_1 - \delta, c_2 - \delta) \ .$$

These operations are equivalent to the AND and EXOR operation on binary signals.
Figure 5a shows a circle rotating at 5 degrees/frame. Obviously, there aren't any occluding regions, and for each point a match can be found. As shown in figure

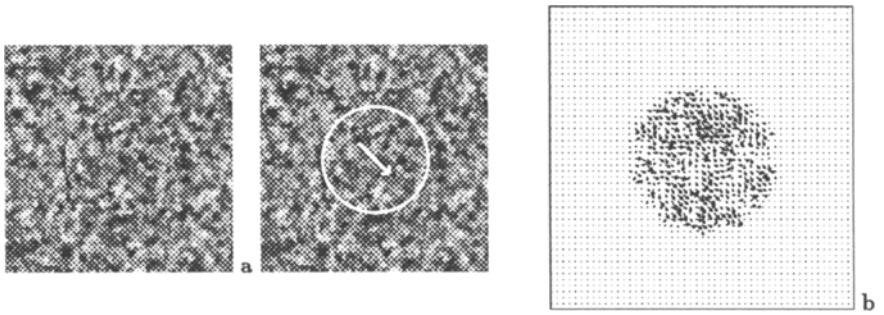

Fig. 3. a: Translating circle. b: Horn & Schunck using 3×3 masks ($\lambda = 0.001$).

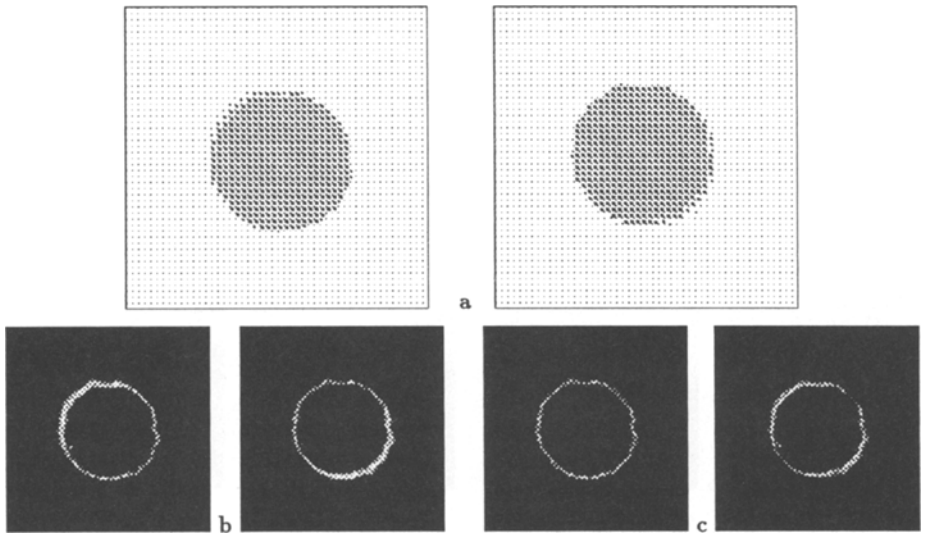

Fig. 4. a: Optic flow fields of the dual scheme ($\lambda = 0.001, K = 0.2, \rho = 0.5, \alpha = 10.0$). b: Inconsistencies c_1 and c_2. c: Boundary δ and occluded regions ω.

6c w is practically non-existent, whereas non-zero values can be accounted for by discretization errors and noise. The 3D plot of figure 5b shows that the velocity magnitude increases linearly from the center to the object boundaries.

Figure 7 shows experiments on a real sequence, a fish moving to the left. The optical flow field is quite reasonable. As for the optical flow boundaries, local thickening can be observed in the inconsistency images, indicating the existence of occluding regions. It must be noted that at some points the inconsistency images are blurred or interrupted. This is due to a lack of contrast with and in the background.

Figure 9 shows a stereo image pair of a shell on a textured background and the resulting disparities. The dips at the center of the shell (figure 10) are due to specular reflections of overhead neon tubes. Such reflections cause problems

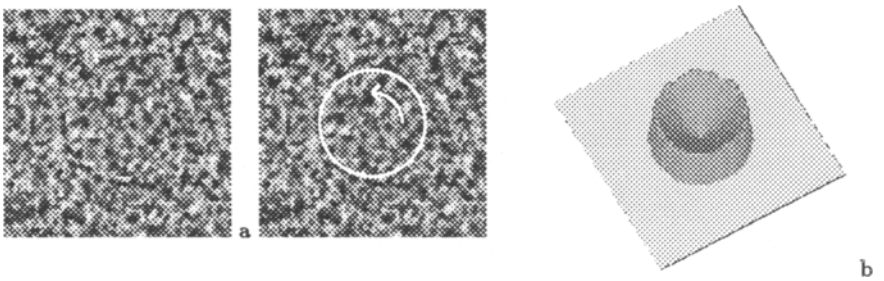

Fig. 5. a: Rotating circle. b: 3-dimensional plot of velocity magnitude.

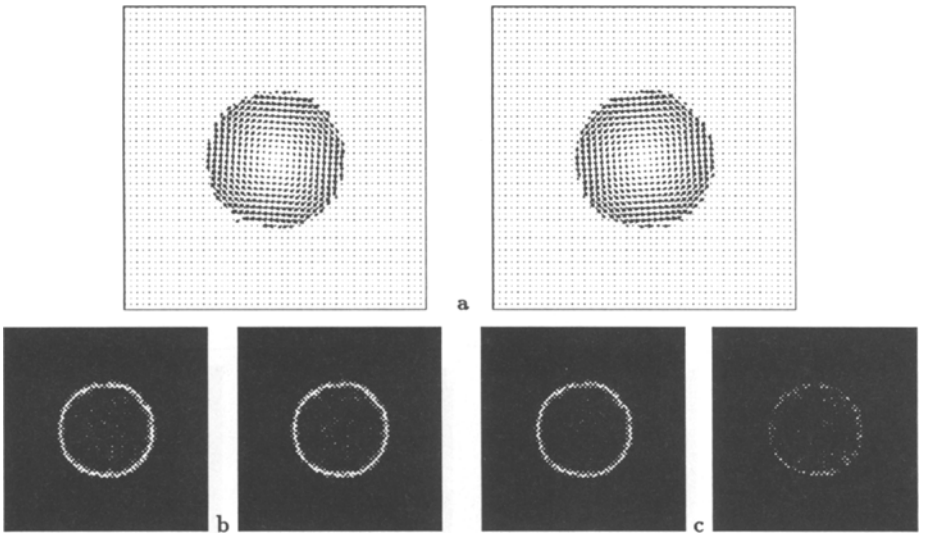

Fig. 6. a: Optic flow fields of the dual scheme ($\lambda = 0.001, K = 0.2, \rho = 0.5, \alpha = 10.0$). b: Inconsistencies c_1 and c_2. c: Boundary δ and occluded regions ω

to stereo. Otherwise, the disparity fields are remarkably smooth, yet sharply delineated. Together with the boundary image (δ) one can reconstruct a depth image while preserving the discontinuity (figure 9b).

8 Conclusions and Future Research

A method was proposed that can be considered a merger of correlation and differential techniques. Although the inclusion of correlation aspects does not really unify the analysis of short-range and long-range motion, a wider range of velocities can be handled without the introduction of larger filters. Therefore the optical flow field can be determined more accurately. A dual scheme has been worked out that provides measures of inconsistency which together indicate the

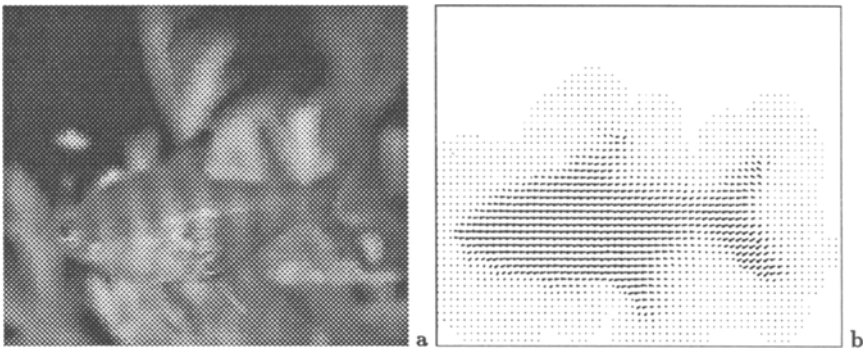

Fig. 7. a: Fish moving to the left. b: Flow field

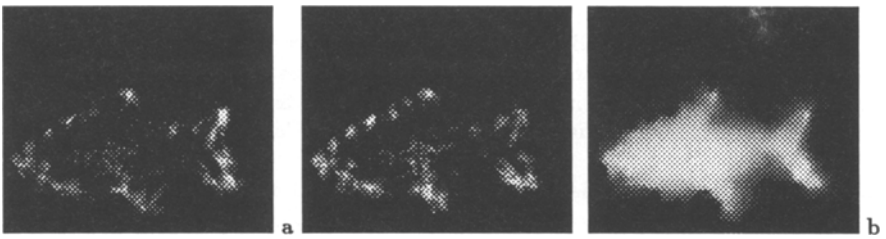

Fig. 8. a: Inconsistencies. b: Segmented image

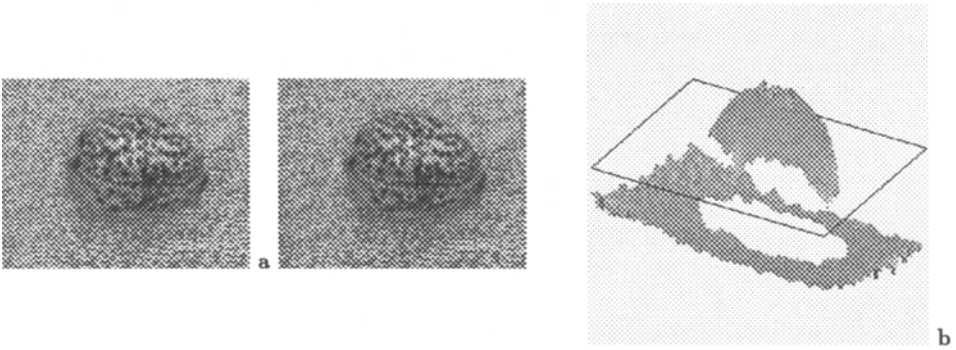

Fig. 9. a: Stereo view of shell on textured background. b: 3D reconstruction.

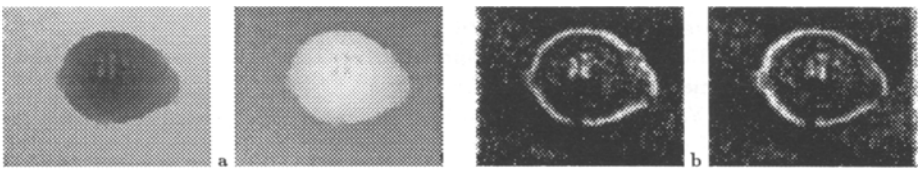

Fig. 10. a: Disparities of left and right scheme. b: Inconsistencies

presence of flow boundaries and occluding regions. Another important aspect of the method is the introduction of non-linearity. It allows to reconstruct the optical flow field preserving its discontinuities.
Ongoing research is aimed at integrating information coming from dual schemes working on different spatial scales. In a further stage the introduction of additional spatio-temporal filters can provide more information about the resulting flow field [14]. Another aspect we intend to address is the problem of changing brightness patterns in time, for which more flexibel motion constraint equations have to be introduced [8].

References

1. Aisbett J.: Optical flow with an intensity-weighted smoothing. IEEE Transactions on PAMI. **11.5** (1989) 512–522
2. Barron J.L., Fleet D.J., Beauchemin S.S., and Burkitt T.A.: Performance of optical flow techniques. IEEE Proceedings of CVPR, Illinois. (1992) 236–242
3. Campani M. and Verri A.: Computing Optical Flow from an Overconstrained Sytem of Linear Algebraic Equations. Proc. Third Int. Conf. on Comp. Vision. Osaka, Japan. (1990) 22–26,
4. Cohen I.: Nonlinear Variational Method for Optical flow computation. Proc. of the 8th Scandinavian Conf. on Image Analysis. **1** (1993) 523–530
5. Horn B.K.P. and Schunck G.: Determining optical flow. Artificial Intelligence. **17** (1981) 185–203
6. Nagel H.H. and Enkelmann W.: An investigation of smoothness constraints for the estimation of displacement vector fields from image sequence. IEEE Transactions on PAMI. **8.5** (1986) 565–593
7. Nagel H.H.: Displacement Vectors Derived from Second-Order Intensity Variations in Image Sequences. Comp. Vision, Graphics, and Image Proc. **21** (1983) 85–117
8. Negahdaripour S. and Yu C.: A generalized Brightness Change Model for Computing Optical Flow. 4th Int. Conf. on Comp. Vision. (1993) 2–11
9. Perona P. and J. Malik J.: Scale-Space and Edge Detection Using Anisotropic Diffusion. IEEE Transactions on PAMI. **12.7** (1990)
10. Pauwels E.J., Proesmans M., Van Gool L.J., T. Moons and Oosterlinck A.: Image Enhancement using coupled anisotropic diffusion equations. Proc. on the 11th European Conf. on circuit theory and design, **2** (1993) 1459–1464
11. Reichardt W.E. and Poggio T.: Figure-ground discrimination by relative movement in the visual system of the fly. Part I: Experimental results. Biological Cybernetics. **35** (1980) 81–100
12. Shah J.: Segmentation by non-linear diffusion. Proc. IEEE CVPR Hawai (1991)
13. Shah J.: (1993) A Nonlinear Diffusion Model for Discontinuous Disparity and Half-Occlusion in Stereo. Proc. IEEE CVPR NY (1993)
14. Weber J. and J. Malik J.: Robust Computation of Optical Flow in a Multi-Scale Differential Framework. 4th Int. Conf. on Comp. Vision. (1993) 12–20
15. Willick D. and Yang Y.: Experimental Evaluation of Motion Constraint Equations. CVGIP: Image Understanding. **54.2** (1991) 206–214